THERMAL ANALYSIS OF CRACKED BODIES USING FINITE ELEMENT TECHNIQUES

T.K. HELLEN, R.H. PRICE, R.P. HARRISON

Central Electricity Generating Board,
Berkeley Nuclear Laboratories, Berkeley, Gloucestershire, United Kingdom

SUMMARY

The calculation of stress intensity factors by finite elements is now a well-established technique. Accurate computational procedures are now available for two and three-dimensional cracked structures. So far, however, nearly all calculation methods, including boundary point collocation, integral equations and closed form solutions, have avoided thermal situations. A variety of methods for calculating stress intensity factors in thermal stress fields is described which are applicable to the finite element method.

The paper develops the potential energy equation in terms of finite element theory including thermal loads. Following this, the energy release rate and consequently the stress intensity factors are derived. Considerations of the classical near crack tip equations are made and deficiencies with the popular substitution methods are highlighted. A method of removing these deficiencies is described.

Various energy methods are reconsidered in terms of the role of the thermal energy contribution to the potential energy. These methods include work of crack closure, energy compliance and virtual crack extensions with no other change in nodal geometry, and therefore only requires the recalculation of the stiffness matrices of the crack tip elements.

An example of a quadratic temperature gradient parallel to the crack plane in an edge cracked plate is described. Comparisons of the various finite element methods are made and generally show good agreement.

A second application compares the virtual crack extension method with an approximate analytical solution in determining stress intensity factors for a thick hollow cylinder with an axial crack for various depths through the wall thickness and for different times. Initially the cylinder is at a uniform high temperature and is then subjected to a sustained cooling shock. Analytical solutions are available for temperature and stress distributions in the uncracked pipe. The stress intensity for a shallow crack in the early stages of the transient has been determined using a superposition procedure. Comparison of the analytical and computed results shows good agreement between the methods.

1. Introduction

Use of the finite element technique to compute stress intensity factors is now well established for mechanically loaded structures. In many instances, however, thermally generated stresses must be taken into account. In the following sections, finite element methods commonly used for evaluating stress intensity factors are assessed in terms of their performance in thermal stress situations. Two numerical examples are then considered in detail. In the first, a single edge-cracked plate with a quadratic thermal distribution is analysed by the various methods and results compared. Secondly, two thick hollow cylinders subjected to a thermal shock are considered using both finite element and analytical techniques.

2. Methods for Calculating Stress Intensity Factors using Finite Elements

2.1 Energy Methods

Stress intensity factors may be obtained from a knowledge of the strain energy release rate, G, given by

$$G = -\frac{d\Pi}{da} \tag{1}$$

for a crack of length a, where Π is the potential energy. Eq. (1) provides the basis for the energy methods for deriving stress intensity factors.

In the finite element method, the basic matrix equation is

$$[K]\{u\} = \{F\} \tag{2}$$

where [K] is the structural stiffness matrix, {u} is the vector of nodal displacements including thermal effects, and {F} is the total equivalent nodal load vector due to mechanical and thermal loads. At every point in the structure, the total strain vector is {ε} where

$$\{\varepsilon\} = \{\varepsilon_e\} + \{\varepsilon_o\} \tag{3}$$

the sum of the mechanical $\{\varepsilon_e\}$ and thermal $\{\varepsilon_o\}$ strains.

The stress vector {σ} is found from the constitutive relations

$$\{\sigma\} = [D](\{\varepsilon\} - \{\varepsilon\}_o) = [D]\{\varepsilon\}_e \tag{4}$$

The compatibility relations at a point are expressed as

$$\{\varepsilon\} = [B]\{u\}^e \tag{5}$$

where $\{u\}^e$ is the vector of displacements at the nodes of the element containing the point and [B] is a matrix depending on the shape function derivatives.

The strain energy density, ρ, is given by

$$\rho = \tfrac{1}{2}(\{\varepsilon\}-\{\varepsilon_o\})^T [D] (\{\varepsilon\}-\{\varepsilon_o\})$$

$$= \tfrac{1}{2}\{\varepsilon\}^T [D] \{\varepsilon\} - \{\varepsilon_o\}^T [D] \{\varepsilon\} + \tfrac{1}{2}\{\varepsilon_o\}^T [D] \{\varepsilon_o\}$$

i.e. $$\rho = \tfrac{1}{2}(\{u\}^e)^T [B]^T [D] [B] \{u\}^e - \{\varepsilon_o\}^T [D] [B] \{u\}^e + \tfrac{1}{2}\{\varepsilon_o\}^T [D] \{\varepsilon_o\} \tag{6}$$

Integrating over the entire structure gives the total strain energy, P, where

$$P = \tfrac{1}{2}\{u\}^T \int [B]^T [D] [B] \, dV\{u\} - \{u\}^T \int [B]^T [D] \{\varepsilon_o\} \, dV + \tfrac{1}{2} \int \{\varepsilon_o\}^T [D] \{\varepsilon_o\} \, dV \quad (7)$$

noting that the {u} vector now applies to the whole structure. The first integral is the stiffness matrix [K]. The potential energy is

$$\Pi = P - \{u\}^T \{F_e\} \quad (8)$$

where $\{F_e\}$ is the vector of mechanical loads. The equivalent thermal load vector is

$$\{F_o\} = \int [B]^T [D] \{\varepsilon_o\} \, dV \quad \text{so that}$$

$$\Pi = \tfrac{1}{2}\{u\}^T [K] \{u\} - \{u\}^T \{F_o\} - \{u\}^T \{F_e\} + \tfrac{1}{2} \int \{\varepsilon_o\}^T [D] \{\varepsilon_o\} \, dV \quad (9)$$

Observe that $$\{F\} = \{F_e\} + \{F_o\} \quad (10)$$

and define $$W = \tfrac{1}{2} \int \{\varepsilon_o\}^T [D] \{\varepsilon_o\} \, dV, \text{ the "thermal energy"} \quad (11)$$

Then $$\Pi = \tfrac{1}{2} \{u\}^T [K] \{u\} - \{u\}^T \{F\} + W$$

$$= -\tfrac{1}{2} \{u\}^T [K] \{u\} + W$$

i.e. $$\Pi = W - V, \text{ say.} \quad (12)$$

V is the strain energy which is obtained in the finite element method using total displacements instead of displacements due to mechanical loads only.

The value of Π may be computed in a variety of ways, but possibly the most efficient is accumulating

$$V = \sum_i \frac{(F_i^*)^2}{k_{ii}^*} \quad (13)$$

in the forward elimination of the Gaussian elimination procedure, F_i^* being the state of the total force component and k_{ii}^* the corresponding stiffness matrix term of the ith degree of freedom at the time when it is eliminated. W is readily accumulated when the element stiffness matrices are assembled, so that Π is known at the end of the forward elimination stage, before any resulting displacements or stresses have been determined.

2.1.1 The Virtual Crack Extension Method (VCE)

If the crack tip - or point along the profile of a crack front in three dimensions - is located at vector position $\underline{a}$, then

$$V(\underline{a}) = \sum_X \frac{(F_i^*(\underline{a}))^2}{k_{ii}^*(\underline{a})} + \sum_A \frac{(F_i^*(\underline{a}))^2}{k_{ii}^*(\underline{a})} \quad (14)$$

where A denotes summation over the crack tip elements and X is over the rest of the structure. If a virtual crack extension is made so that the tip is displaced to $\underline{a} + \underline{\delta a}$,

$$V(\underline{a}+\underline{\delta a}) = \sum_X \frac{(F_i^*(\underline{a}+\underline{\delta a}))^2}{k_{ii}^*(\underline{a}+\underline{\delta a})} + \sum_B \frac{(F_i^*(\underline{a}+\underline{\delta a}))^2}{k_{ii}^*(\underline{a}+\underline{\delta a})} \quad (15)$$

B denoting summation over the new crack tip domain.

The virtual extension involves no changes of geometry or load in X, so in eq. (14) and eq. (15) the summations over X are equal, and

$$\delta V = V(\underline{a}+\underline{\delta a}) - V(\underline{a})$$

$$\text{i.e.} \quad \delta V = \sum_{B} \frac{(F_i^*(\underline{a}+\underline{\delta a}))^2}{k_{ii}^*(\underline{a}+\underline{\delta a})} - \sum_{A} \frac{(F_i^*(\underline{a}))^2}{k_{ii}^*(\underline{a})} \tag{16}$$

In a similar manner, the thermal energy W is invariant in elements away from the crack tip so that if $W(\underline{a})$ and $W(\underline{a}+\underline{\delta a})$ are the thermal energy accumulations over the crack tip elements with the tip at $\underline{a}$ and $\underline{a}+\underline{\delta a}$ respectively, we have

$$\delta W = W(\underline{a}+\underline{\delta a}) - W(\underline{a}) \tag{17}$$

$$\text{and} \quad \delta \Pi = \Pi(\underline{a}+\underline{\delta a}) - \Pi(\underline{a})$$

$$= -V(\underline{a}+\underline{\delta a}) + V(\underline{a}) + W(\underline{a}+\underline{\delta a}) - W(\underline{a})$$

$$\text{i.e.} \quad \delta \Pi = \delta W - \delta V \tag{18}$$

Hence an approximation to

$$G = -\frac{d\Pi}{da} = \frac{dV}{da} - \frac{dW}{da} \tag{19}$$

is readily obtained from scalar quantities δV and δW accumulated only over the tip elements. If the order of elements is such that, in the forward elimination, the crack tip elements are treated last of all, it is possible to retrace the elimination procedure, and therefore the accumulation of δV and δW, with the tip node moved slightly. Thus the difference in Π for a corresponding value δa is obtained. Several such repetitions may be made in succession, each (after the first) giving an independent result for any reasonable crack extension in any direction. The method works equally well for two and three dimensional structures[2].

An efficient method is therefore available from eq. (19) for calculating the instantaneous energy release rate and thus the stress intensity factors K_I, K_{II}, and K_{III}, given by

$$G = \frac{(1-\nu^2)}{E}(K_I^2 + K_{II}^2) + \frac{(1+\nu)}{E} K_{III}^2 \quad \text{(plane strain)}$$

$$\text{or} \quad G = \frac{1}{E}(K_I^2 + K_{II}^2 + K_{III}^2) \quad \text{(plane stress)} \tag{20}$$

where ν is Poisson's ratio and E is Young's modulus, for an arbitrary structure in two or or three dimensions with mechanical and thermal loading.

This method is available in the BERSAFE system[3], where such facilities as multi-case loadings and decoupling of degrees of freedom between different elements are still applicable. The extra computing costs add only a few percent and, if the calculation of displacements and stresses in the back substitution process is not required, the cost can be less than that of a normal run. No extra arrays of storage are involved. In addition, the total potential energy of the whole structure (eq. (12)) may be produced, whether the

virtual crack extension method is used or not.

2.1.2 Energy Difference Technique

From calculation of Π at a series of crack tip positions, the derivative $\frac{d\Pi}{da}$ can be obtained as a function of crack length, a. Then using eq. (1) and eq. (20), it is possible to define the stress intensity factor as a function of crack length. It will be noted that two computer submissions are required even if only one crack length is being studied.

2.1.3 Crack Closure Work

This method, described by Jerram[4] uses the multi-loading case facility offered by most finite element computer programs. The first case has the required loading system, and the second has an extra load of unity applied at the first vertex node along the crack in a direction to close the crack. From the results, it is possible to find the force P at the vertex to close the crack completely at the vertex. The work done by this force is $\frac{1}{2}P\delta$ (δ being the closure) which, when divided by δa, the length of crack closed, gives the energy release rate G for a crack of approximate length $a + \frac{1}{2}\delta a$. As described, a K_I mode is implied, the other modes being effected by independent unit loads in the required directions. So in a mixed mode case, the individual stress intensity factors can be derived.

The above refers to elements with only vertex nodes. The method is readily extended to elements with additional nodes along the element sides using extra loading cases.

In thermal cases, the method applies since the displacement, δ, includes no thermal contributions as it arises entirely from the force P. Consequently, the work done term may be used directly to find the energy release rate.

2.1.4 Bueckner's Formulation

Bueckner[5] demonstrated that the rate of change of strain energy with crack length in a loaded body is the same as the rate of change of work done by tractions acting on the surface defining the position of the crack when the crack was absent from the body. Hayes[6] has utilised this method for several mechanically-loaded geometries and found good accuracy. The method applies for thermal loading because, as in the previous case, the work terms are due entirely to mechanical loads.

2.1.5 J-Integral Method

Rice[7] demonstrated that the value of the line integral

$$J = \int_{\Gamma} (\Omega dy - T_i \frac{\partial u_i}{\partial x} ds)$$

is path independent along any contour Γ surrounding the crack tip, and equals G. Here, $\Omega = \Omega(\varepsilon_e)$ is the strain energy density, T_i are components of traction, u_i are components of displacement, s is a measure of length along the contour, and i denotes summation.

Unfortunately, when thermal strains are present, J ceases to be path independent. This is easily shown by writing $\varepsilon^e_{ij} = \varepsilon^T_{ij} - \varepsilon^o_{ij}$, i.e. total strain less thermal strain at a point, and considering a complete contour defined by two non-coincident contours around the crack tip and the sections of crack connecting their ends.

By Green's theorem, defining S as the area enclosed by this complete contour, a value for the integral, J', is obtained:

$$J' = \iint \{\frac{\partial \Omega}{\partial x} - \frac{\partial}{\partial x_j} (\sigma_{ij} \frac{\partial u_i}{\partial x})\} \, dS$$

Now $\Omega = \Omega (\varepsilon^e_{ij})$ so $\frac{\partial \Omega}{\partial x} = \frac{\partial \Omega}{\partial \varepsilon^e_{ij}} \cdot \frac{\partial \varepsilon^e_{ij}}{\partial x} = \sigma_{ij} \frac{\partial \varepsilon^e_{ij}}{\partial x}$ and

$$J' = \iint \{\sigma_{ij} \frac{\partial \varepsilon^T_{ij}}{\partial x} - \sigma_{ij} \frac{\partial \varepsilon^o_{ij}}{\partial x} - \sigma_{ij} \frac{\partial^2 u_i}{\partial x \partial x_j}\} \, dS \quad \text{by equilibrium}$$

$$= \iint \{\sigma_{ij} \frac{\partial \varepsilon^T_{ij}}{\partial x} - \sigma_{ij} \frac{\partial \varepsilon^o_{ij}}{\partial x} - \sigma_{ij} \frac{\partial \varepsilon^T_{ij}}{\partial x}\} \, dS$$

i.e. $$J' = - \iint \sigma_{ij} \frac{\partial \varepsilon^o_{ij}}{\partial x} \, dS$$

Thus $J' = 0$, i.e. J is path independent, only if the thermal strain is constant in the x-direction. The integral may be modified to give $J' = 0$, by defining

$$J^* = \int_\Gamma (\Omega dy - T_i \frac{\partial u^e_i}{\partial x} \, ds),$$

where u^e_i are displacement components with no thermal contributions. However, as $\Gamma \to 0$, the value of J^* does not tend to a physically meaningful energy release rate.

2.2 Substitution in the Classical Crack Tip Equations

Define a system of polar and cartesian coordinates with origin at the crack tip and $\theta = 0^o$ along a projection of the crack in the uncracked material. Let u be the displacement along $\theta = 0^o$ and v be the displacement along $\theta = 90^o$. Then the classical Westergaard crack tip equations are

$$u = \frac{1+\nu}{4E} \sqrt{\frac{2r}{\pi}} \{K_I [(2\kappa-1) \cos \frac{\theta}{2} - \cos \frac{3\theta}{2}] + K_{II} [(2\kappa+3) \sin \frac{\theta}{2} + \sin \frac{3\theta}{2}]\} \qquad (21)$$

and similarly for v, and

$$\sigma_x = \frac{1}{\sqrt{2\pi r}} \{K_I \cos \frac{\theta}{2} (1 - \sin \frac{\theta}{2} - \sin \frac{3\theta}{2}) - K_{II} \sin \frac{\theta}{2} (2 + \cos \frac{\theta}{2} - \cos \frac{3\theta}{2})\} \qquad (22)$$

and similarly for the other stress components. Here,

$\kappa = 3 - 4\nu$ for plane strain and $(3-\nu)/(1+\nu)$ for plane stress.

In mechanical loading cases, this method has been used frequently in conjunction with finite element analysis (Chan et al[8]). It has been found that for different points around the crack tip, there is some scatter in the stress intensity results. In thermal cases, however, the displacements include thermal effects, and around the crack tip such effects are important enough to render direct substitution in eq. (21) inaccurate. While no such difficulty should exist in the use of eq. (22), experience has shown that stress intensity values so obtained are less accurate than those obtained by substitution in eq. (21).

A method of overcoming this difficulty in eq. (21) is to eliminate the unwanted thermal strain using two applications, at points (h, θ) and (2h, θ), where the former is a midside node and the latter is a vertex node in a special 6-node triangular crack tip element. This 'special element' differs from the usual quadratic isoparametric element in that it has an imposed displacement function in the radial direction from the tip as

$$u = a_1 + (a_2\xi + a_3\eta + a_4\xi\eta)/\sqrt{(\xi + \eta)} + a_5\xi + a_6\eta \qquad (23)$$

where ξ and η are dimensionless coordinates inside the element[9]. If K_M and K_V are obtained from substitution in equation (21) at (h, θ) and (2h, θ), respectively, then

$$K^* = K_V + (2 + \sqrt{2})\ (K_M - K_V) \qquad (24)$$

gives a value for stress intensity from which the constant strain terms of eq. (21) have been eliminated. Note that eq. (24) holds for any mode.

3. Assessment of Methods for a Thermally-Loaded Edge-Cracked Plate

The procedures described above were compared by using them to determine stress intensity factors for a rectangular single edge-cracked plate 250 mm wide by 500 mm long, subjected to a temperature distribution given by

$$T = 50 + 2.8x - 0.0064x^2$$

where x was the distance measured parallel to the crack plane, see inset fig. 1. For computing purposes only half of the plate was modelled because of symmetry about the crack plane. There were 110 8 noded quadrilateral isoparametric elements in the basic finite element mesh. Near the crack tip the mesh was refined by the insertions of extra 6 noded triangular elements, either the normal isoparametric type or special crack tip singularity elements. Three degrees of refinement were used with element sizes around the crack tip of 25, 12.5 or 6.25 mm, referred to as coarse medium or fine, respectively. A crack length of 50 mm was selected and mathematical plane strain conditions were assumed throughout.

Results using the VCE method are shown in Table I. As the mesh was refined, the K values increase but seem to converge. Ordinary elements around the crack tip gave results up to 6% higher than special elements. This difference was less for the coarse mesh and is currently being investigated. The value of crack extension used had little effect.

The crack closure work method needed three independent load cases, because of the presence of midside nodes, with point loads suitably scaled to close the crack. The results, Table I, show that the fine mesh gave 66 $MN.m^{-3/2}$ with and 62 $MN.m^{-3/2}$ without special crack tip elements.

The results from the potential energy difference and Bueckner methods were identical and are therefore combined in Table I. They were only slightly different from those obtained using the crack closure work method.

Computed displacements were substituted in the relevant Westergaard crack tip equation to determine the stress intensities shown in Table I. Values for K_M and K_V are given for θ = 90° and 180° (using eq. 21), where M and V denote midside and vertex nodes away

from the crack tip respectively, i.e. different distances from the crack tip. The value of K^* was found from eq. (24) and, as expected, varies widely due to the incomplete nature of eq. (21), particularly for the normal isoparametric crack tip elements.

Subsequently the variation of stress intensity with crack length was computed using VCE and crack closure methods, the former with and without special elements and using the medium mesh. The results are shown in Fig. 1 where comparison is also made with some results produced by Chell[10] using the uncracked body stresses and a technique described by Chell[11]. Good agreement is seen between the different methods particularly for longer crack lengths.

4. Stress Intensity Factors for Thermally Shocked Cylinders

Two long circular cylinders were considered, one representing a pipe, inside radius 350 mm and 63 mm thick, the other a large vessel 2200 mm inside radius and 215 mm wall thickness. In both cases, the bodies were at a uniform high temperature initially, and then subjected to sustained rapid cooling of the inside. The magnitude of the temperature difference between the cooled inside surface and the outside was 270 deg. C.

The temperature response was calculated using the finite element program FLHE[12]. A plane-strain two-dimensional analysis was then carried out to determine the stresses and stress intensity factors for a part-through radial crack using the VCE method with special crack tip elements. The calculations were repeated for numerous times during the transient and for various depths of crack (figs. 2 and 3). Some computations were repeated without special elements and maximum differences of the order of 5% were found in the stress intensity factors.

Analytical solutions for the temperature distribution are given by Carslaw and Jaeger[13] in the form of a series involving the error function and its integrals. Only the first term in the series need be considered if the analysis is restricted to short times. The stress distribution in an uncracked cylinder can be derived formally from the temperature distribution[14]. Emery[15] has used these well-known results and derived formulae for stress intensity factors for thermal shocks in thick cylinders using approximate solutions for a semi-infinite edge-cracked plate and assuming linear superposition. When the shock takes the form of a sudden cooling of the inside surface, Emery's solution is

$$\frac{K_I}{\sqrt{a}} = 1.95\,\sigma_\theta - 1.18\,\frac{a}{w}\,\frac{E\alpha|\Delta T|}{1-\nu}\left[\frac{6}{\sqrt{\pi}}\sqrt{\frac{t_{max}}{t}} + \left\{\frac{\sigma_\theta(1-\nu)}{E\alpha|\Delta T|} + 0.5\right\}\delta\right] \qquad (25)$$

where α is the coefficient of thermal expansion.

$|\Delta T|$ is the magnitude of the temperature shock.

t is the time since the thermal shock was initiated.

$\delta = r_o/r_i - 1$ where r_i and r_o are the cylinder inside and outside radii.

w = wall thickness = $r_o - r_i$.

σ_θ = hoop stress at the inside surface of the uncracked cylinder.

For the approximated temperature distribution to be accurate

$$\delta \le 0.4 \qquad (26)$$

$$t \le t_{max}. \qquad (27)$$

where t_{max} is given by $\sqrt{kt_{max}} = (r_o - r_i)/6$

and k is the thermal diffusivity of the material.

The stress intensity calculations were further restricted by the requirement that

$$a \leq 0.2\ L \qquad (28)$$

where L is the depth from the inside surface to the point where the hoop stress is zero in the uncracked cylinder.

For the pipe $\delta = 0.18$, so condition (26) is satisfied. Eq. (27) gives a value of 10 sec. for t_{max}. At t = 10 sec., L is 18 mm, so the maximum crack depth from eq. (28) is 3.6 mm. Computed results for the hoop stress (σ_θ) in the uncracked body have been used instead of approximate analytical values. This enables Emery's approach to be extended to much longer times. Values of K_I obtained by substitution in eq. (25) are shown in fig. 2. There is excellent agreement with VCE for a = 3.6 mm. For deeper cracks (e.g. a = 10.4 mm), Emery's formula is not strictly applicable, and although the variation of K_I with time is similar to the computed VCE curve, the level is significantly lower.

For the vessel, the smallest crack considered was 3.3 mm. Emery's conditions are satisfied for $5 \leq t \leq 120$ sec. and good agreement is observed with the VCE results. For the middle curve of fig. 3, a = 19.9 mm, condition (28) is not satisfied but there is still good correlation except at t = 10 sec. The upper curve shows VCE results for a much deeper crack (a = 57 mm) but this is too far beyond the limits for the Emery solution to be used.

5. Conclusions

Several methods for computing stress intensity factors, using finite elements, have been examined. It has been shown that suitable modifications have to be made to extend these methods from mechanical to thermal load situations. Consistent results, within 7%, have been obtained between the virtual crack extension, crack closure work, energy difference, and Bueckner methods using normal quadratic isoparametric elements around the crack tip. For practical purposes, this is clearly adequate. However, when using special crack tip elements, rather larger deviations occurred warranting further investigation. The substitution methods gave widely varying results. This variation appears worse than for mechanical loading cases and is due to thermal displacements not being properly accounted for in the crack tip equations.

Acknowledgement

This paper is published by permission of the Central Electricity Generating Board.

TABLE I

Results for Single Edge-Cracked Plate with Quadratic Thermal Gradient

Method		Mesh without Special Crack Tip Elements			Mesh with Special Crack Tip Elements		
		Coarse	Medium	Fine	Coarse	Medium	Fine
Virtual Crack Extension		48.82	56.29	57.97	49.14	52.95	54.88
Crack Closure Work				62.35			66.04
Change in Potential Energy - Bueckner				62.33			66.05
Substitution							
$\theta = 90^{o}$	K_M	121	97	79	163	131	107
	K_V	168	134	108	203	158	126
	K^*	9	9	10	67	65	60
$\theta = 180^{o}$	K_M	62	58	56	73	64	59
	K_V	73	66	61	84	70	64
	K^*	35	41	43	47	48	48

References

[1] HELLEN, T.K., "On the Method of Virtual Crack Extensions", Int. J. Numer. Meths. Eng'g. 9, 187-207 (1975).

[2] HELLEN, T.K., DOWLING, A.R., "Three Dimensional Crack Analysis Applied to an LWR Nozzle-Cylinder Intersection", Int. J. Press. Vessels and Piping, 3, 57-74 (1975).

[3] HELLEN, T.K., PROTHEROE, S.J., "The BERSAFE Finite Element System", Computer Aided Design, 6, 15-24 (1974).

[4] JERRAM, K., Discussion of paper by Smith and Alari, Int. Conf. on Pressure Vessel Technology, Part III Discussion, ASME, New York, 1970.

[5] BUECKNER, H.F., "Propagation of Cracks and the Energy of Elastic Deformation", Trans. ASME, 80, 1225-1229 (1958).

[6] HAYES, D.J., "A Practical Application of Bueckner's Formulation for Determining Stress Intensity Factors for Cracked Bodies", Int. J. Frac. Mechs., 8, 157-166 (1972).

[7] RICE, J.R., "A Path Independent Integral and the Approximate Analysis of Strain Concentration by Notches and Cracks", J. Appl. Mechs., 35, 379-386 (1968).

[8] CHAN, S.K., TUBA, I.S., WILSON, W.K., "On the Finite Element Method in Linear Fracture Mechanics", Eng. Fract. Mechs., 2, 1-17 (1970).

[9] BLACKBURN, W.S., "Calculation of Stress Intensity Factors at Crack Tips using Special Finite Elements", Conf. Maths of Fin. Els. and Applications, Brunel University, England (1972).

[10] CHELL, G.G., Private Communication (1974).

[11] CHELL, G.G., Engng. Fracture Mechanics, to be published, 1975.

[12] FULLARD, K., "The Computation of Temperature Distributions and Thermal Stress using Finite Element Techniques", S.M.i.R.T. 1st Conf., Paper M5/3, Berlin, September 1971.

[13] CARSLAW, H.S., JAEGER, J.C., Conduction of Heat in Solids, Oxford Press 1959.

[14] TIMOSHENKO, S.P., GOODIER, J.N., Theory of Elasticity, Eng. Soc. Monographs (3rd Ed.) 1970.

[15] EMERY, A.F., "Stress Intensity Factors for Thermal Stresses in Thick Hollow Cylinders" J. Basic Engng., 45-52, 1966.

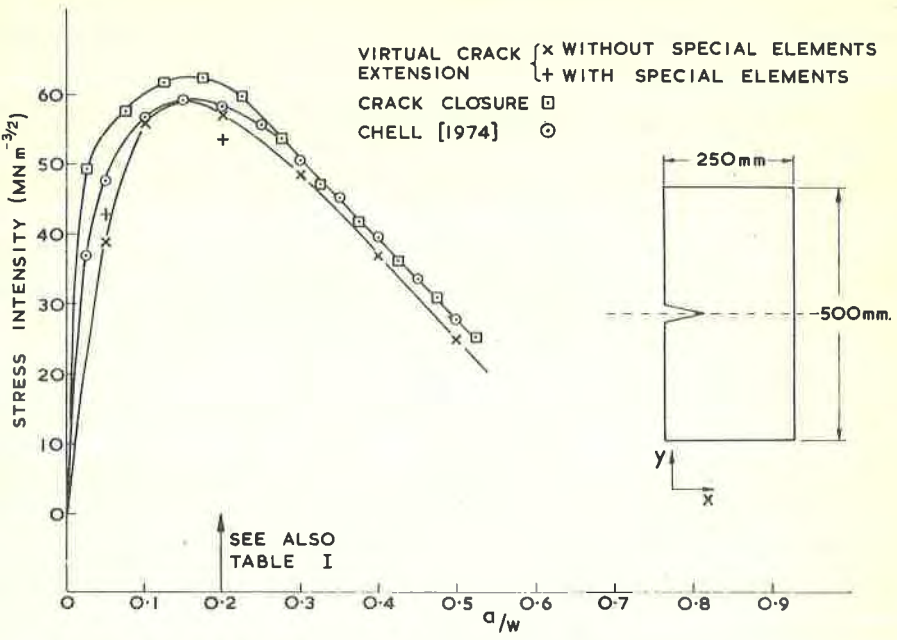

Fig. 1 Stress intensity factors for a single edge notched plate subjected to a quadratic thermal gradient.

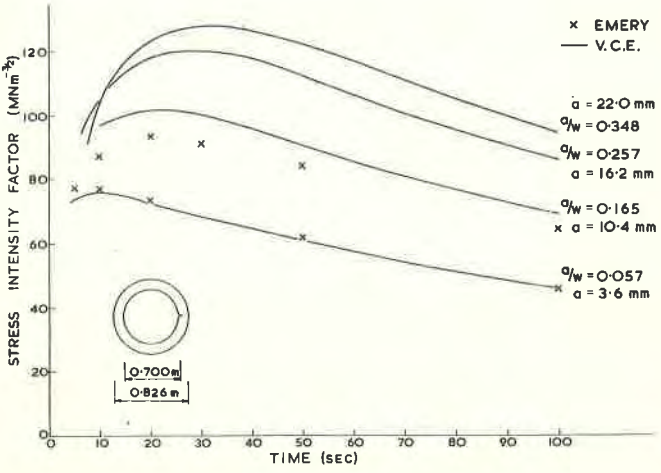

Fig. 2 Stress intensity factors for a pipe subject to a sustained thermal shock.

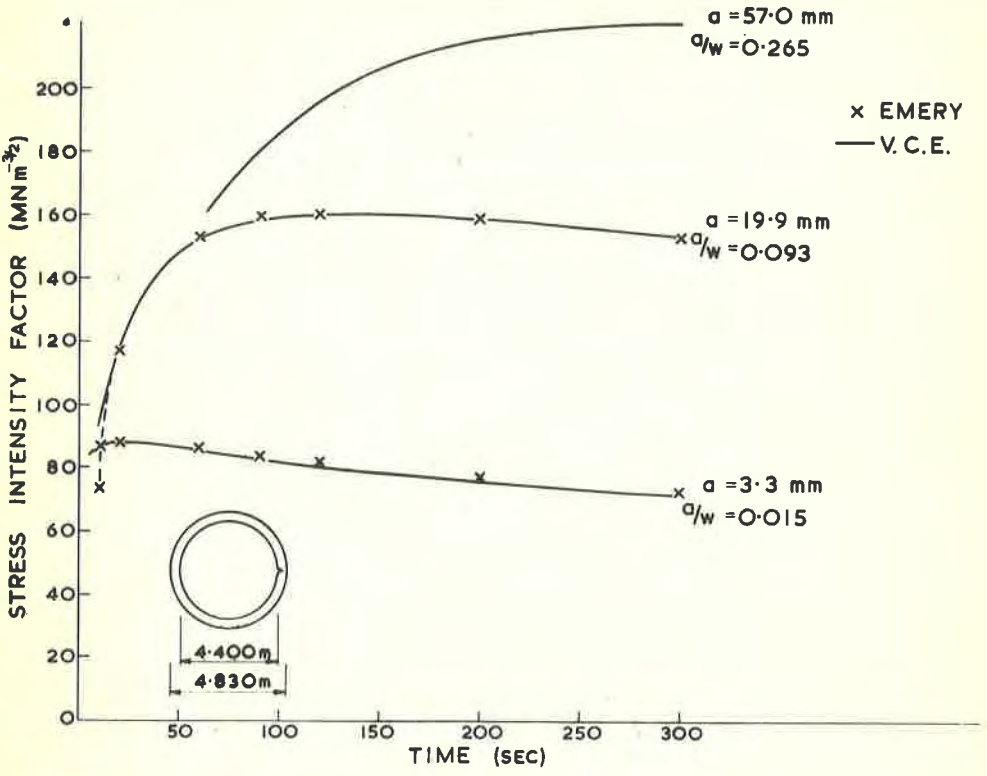

Fig. 3 Stress intensity factors for a vessel subject to a sustained thermal shock.